Light meson spectroscopy with the KLOE experiment.

The KLOE Collaboration

A. Aloisio [g], F. Ambrosino [g], A. Antonelli [c], M. Antonelli [c], C. Bacci [m], M. Barva [m], G. Bencivenni [c], S. Bertolucci [c], C. Bini [k], C. Bloise [c], V. Bocci [k], F. Bossi [c], P. Branchini [m], S. A. Bulychjov [f], R. Caloi [k], P. Campana [c], G. Capon [c], T. Capussela [g], G. Carboni [ℓ], F. Ceradini [m], F. Cervelli [i], F. Cevenini [g], G. Chiefari [g], P. Ciambrone [c], S. Conetti [o], E. De Lucia [k], A. De Santis [k], P. De Simone [c], G. De Zorzi [k], S. Dell'Agnello [c], A. Denig [d], A. Di Domenico [k], C. Di Donato [g], S. Di Falco [i], B. Di Micco [m] A. Doria [g], M. Dreucci [c], O. Erriquez [a], A. Farilla [m], G. Felici [c], A. Ferrari [m], M. L. Ferrer [c], G. Finocchiaro [c], C. Forti [c], P. Franzini [k], C. Gatti [k], P. Gauzzi [k], S. Giovannella [c], E. Gorini [e], E. Graziani [m], M. Incagli [i], W. Kluge [d], V. Kulikov [f], F. Lacava [k], G. Lanfranchi [c] J. Lee-Franzini [c,n], D. Leone [k], F. Lu [c,b], M. Martemianov [c], M. Martini [c], M. Matsyuk [c], W. Mei [c], L. Merola [g], R. Messi [ℓ], S. Miscetti [c], M. Moulson [c], S. Müller [d], F. Murtas [c], M. Napolitano [g], F. Nguyen [m], M. Palutan [c], E. Pasqualucci [k], L. Passalacqua [c], A. Passeri [m], V. Patera [c,j], F. Perfetto [g], E. Petrolo [k], L. Pontecorvo [k], M. Primavera [e], P. Santangelo [c], E. Santovetti [ℓ], G. Saracino [g], R. D. Schamberger [n], B. Sciascia [c], A. Sciubba [c,j], F. Scuri [i], I. Sfiligoi [c], A. Sibidanov [c,h], T. Spadaro [c], E. Spiriti [m], M. Testa [k], L. Tortora [m], P. Valente [c], B. Valeriani [d], G. Venanzoni [c], S. Veneziano [k], A. Ventura [e], R.Versaci [m], I. Villella [g], G. Xu [c,b]

[a] *Dipartimento di Fisica dell'Università e Sezione INFN, Bari, Italy.*

[b] *Permanent address: Institute of High Energy Physics, CAS, Beijing, China.*

[c] *Laboratori Nazionali di Frascati dell'INFN, Frascati, Italy.*

[d] *Institut für Experimentelle Kernphysik, Universität Karlsruhe, Germany.*

[e] *Dipartimento di Fisica dell'Università e Sezione INFN, Lecce, Italy.*

[f] *Permanent address: Institute for Theoretical and Experimental Physics, Moscow, Russia.*

[g] *Dipartimento di Scienze Fisiche dell'Università "Federico II" e Sezione INFN, Napoli, Italy*

[h] *Permanent address: Budker Institute of Nuclear Physics, Novosibirsk, Russia*

[i] *Dipartimento di Fisica dell'Università e Sezione INFN, Pisa, Italy.*

[j] *Dipartimento di Energetica dell'Università "La Sapienza", Roma, Italy.*

[k] *Dipartimento di Fisica dell'Università "La Sapienza" e Sezione INFN, Roma, Italy.*

[ℓ] *Dipartimento di Fisica dell'Università "Tor Vergata" e Sezione INFN, Roma, Italy.*

[m] *Dipartimento di Fisica dell'Università "Roma Tre" e Sezione INFN, Roma, Italy.*

[n] *Physics Department, State University of New York at Stony Brook, USA.*

[o] *Physics Department, University of Virginia, USA.*

Abstract

We describe the status of the analyses in progress on light meson spectroscopy in the KLOE experiment. We present the analyses of ϕ decays into $f_0(980)\gamma$ and $a_0(980)\gamma$, the Dalitz plot analysis of the $\eta \to \pi^+\pi^-\pi^0$ decay, the branching ratio measurement of $\eta \to \pi^0\gamma\gamma$, the upper limits on $Br(\eta \to 3\gamma)$ and $Br(\eta \to \pi^+\pi^-)$, the measurement of the ratio $Br(\phi \to \eta'\gamma)/Br(\phi \to \eta\gamma)$ and ϕ leptonic width measurements.

1 Introduction

The KLOE detector [1–4], operates at the Frascati e^+e^- collider DAΦNE [5], which runs at a CM energy W equal to the ϕ-meson mass, $W\sim$1019.5 MeV. The highest ϕ-production rate that has been obtained up to 2002 was $\sim$ 240 ϕ/s, in October 2002. The analyses presented here are based on data collected in the years 2001 and 2002 for an integrated luminosity of $\sim$ 450 pb^{-1}.

The KLOE detector consists of a large cylindrical drift chamber [1], DC, surrounded by a lead/scintillating-fiber sampling calorimeter [2], EMC, both immersed in a solenoidal magnetic field of 0.52 T with the axis parallel to the beams. Two small calorimeters [3] are wrapped around the quadrupoles of the low-β insertion to complete the detector hermeticity. The DC provides a measurement of charged tracks momentum with a resolution of $\delta p_\perp/p_\perp$=0.4%, and of decay vertices with an accuracy of 3 mm. The calorimeter covers 98% of the total solid angle and provides measurements of energy, time and position of photons with accuracies of $\sigma_E/E = 0.057/\sqrt{E\ (\mathrm{GeV})}$ and $\sigma_t = 54\ \mathrm{ps}/\sqrt{E\ (\mathrm{GeV})} \oplus 50$ ps, respectively. A photon is defined as a cluster of energy deposits in the calorimeter not associated to a charged particle.

The trigger [4] uses information from both the calorimeter and the drift chamber. The EMC trigger requires two local energy deposits while the DC trigger is based on the multiplicity and topology of the hits in the drift cells.

In this paper we describe the analyses of ϕ in light meson spectroscopy using the KLOE detector: the ϕ decays to scalar mesons $\phi \to f_0\gamma$, $\phi \to a_0\gamma$, the decays of the η meson in charged and neutral particles, the ϕ decay into η, η' mesons, and finally the ϕ leptonic width measurement.

2 ϕ radiative decays to scalar mesons.

2.1 Introduction.

The ϕ radiative decays to scalar mesons, $\phi \to$Sγ, give significant insight in the assessment of the nature of lower mass scalar mesons [6]. The scalar iso-scalar mesons (the $\mathrm{f_0}(980)$ and possibly the σ) are searched for in $\pi^0\pi^0\gamma$, $\pi^+\pi^-\gamma$ final states, and the scalar iso-vector $a_0(980)$ in $\eta\pi^0\gamma$ states.

KLOE has already published analyses of $\eta\pi^0\gamma$ [7] and of $\pi^0\pi^0\gamma$ [8] final states, based on a data sample of about 17 pb^{-1} collected in year 2000. Several fits have been performed on these data, using different theoretical approaches [9]. Here we present preliminary results based on the considerably larger data sample collected in 2001 and 2002. We have extended our analysis to the $\pi^+\pi^-$ channel, where the presence of a huge irreducible background requires a large data sample.

2.2 $\eta\pi^0\gamma$ final states.

$\eta\pi^0\gamma$ final states are selected through the decay chains $\eta \to \gamma\gamma$ and $\eta \to \pi^+\pi^-\pi^0$. In the first case the final state is fully neutral with 5 calorimeter clusters and no tracks; in the second case there are 2 tracks and 5 neutral calorimeter clusters. About 23000 (5000) events have been selected for the first (second) decay chain. The preliminary branching ratio obtained from the two channels are:

$$B.R.(\phi \to \eta\pi^0\gamma) = (7.25 \pm 0.15) \times 10^{-5} \quad \text{from } \eta \to \gamma\gamma$$

$$B.R.(\phi \to \eta\pi^0\gamma) = (7.45 \pm 0.19) \times 10^{-5} \quad \text{from } \eta \to \pi^+\pi^-\pi^0$$

The two $\eta\pi^0$ invariant mass spectra (see Fig.1) are characterized by a broad asymmetric peak in the high mass region due to the a_0 contribution and by a smooth tail in the low mass region. The two distributions are fitted simultaneously to a model describing the ϕ to scalar decay through a charged kaon loop [10]. Free parameters of the fit are: the a_0 mass, the two couplings g_{a_0KK} and $g_{a_0\eta\pi}$, the size of the $\phi \to \rho^0\pi^0 \to \eta\gamma\pi^0$ contribution [1] and the relative phase δ between the a_0 and the $\rho\pi$ terms. A good fit is obtained only setting to a value compatible with 0 the $\rho\pi$ contribution. This is an unexpected result, since the $\rho\pi$ contribution should be observable. It could signal an inconstency in the used parametrization. Neglecting the $\rho\pi$ term, the a_0 term alone well describes the two spectra as shown in fig.1; the a_0 parameters are in agreement with the results of the fit done on the 2000 data sample [7]. In fig.2 the Dalitz plot of the a_0 decay is shown.

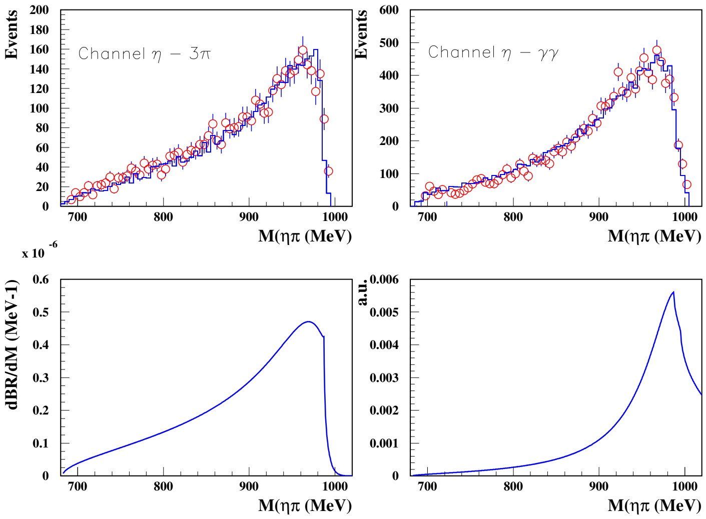

Fig. 1. **Top**: $\eta\pi^0$ invariant mass spectra (red points) for the $\eta \to \pi^+\pi^-\pi^0$ (left) and $\eta \to \gamma\gamma$ (right) samples. The fit overimposed is obtained by convoluting the theoretical functions with the estimated efficiencies and resolutions. **Bottom**: line shape of the resulting theoretical functions (left) completely due to the a_0 term, and (right) the a_0 contribution as it appears once the E_γ^3 dependence due to the ϕ radiative decay dynamic is taken away.

[1] This contribution is assumed to follow the mass shape given in [10,11]

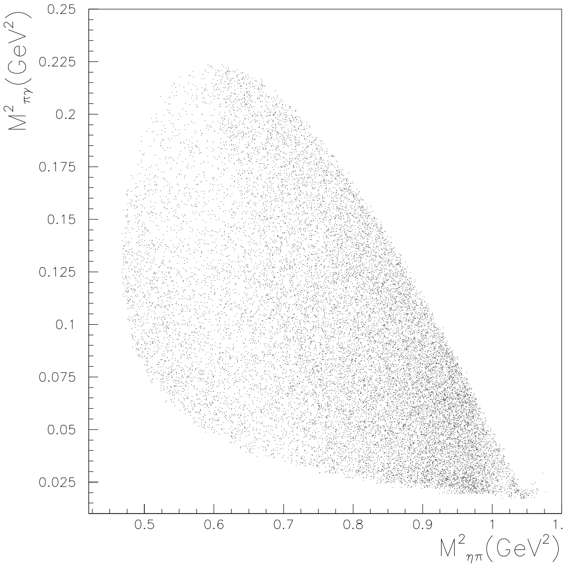

Fig. 2. Dalitz plot of the $\phi \to \eta(\to \gamma\gamma)\pi^0\gamma$ decay; the events outside the allowed region at high $M(\eta\pi^0)$ are due to residual background from $\phi \to \eta(\to \gamma\gamma)\gamma$.

2.3 $\pi^0\pi^0\gamma$ *final states.*

$\pi^0\pi^0\gamma$ final states are selected by looking for neutral events with 5 calorimeter clusters satisfying a kinematic fit constraining energy momentum conservation and the 2 π^0 messes. About 1.5×10^5 events have been selected at the ϕ peak. The distribution of these events in the allowed phase-space region is shown in the Dalitz plot of fig.3. The two sharp bands correspond to $e^+e^- \to \omega(\to \pi^0\gamma)\pi^0$, while the structure close to the high $M^2_{\pi\pi}$ corner is due to $\phi \to$f$_0(\to \pi^0\pi^0)\gamma$. Fig.4 (bottom half) shows the visible cross-sections of the events in the $\omega\pi^0$ bands and (top half) the remaining part of the Dalitz plot respectively, as a function of $\sqrt{s}$. A clear ϕ resonant behavior is observed for the f$_0$ events, while a negative interference between the smooth dependence of the $\omega\pi^0$ continuum and the isospin violating decay $\phi \to \omega\pi^0$ is observed for the $\omega\pi^0$ events.

An overall fit of these data is in progress, with the aim of extracting the f$_0$ parameters taking into account all the possible interferences of the f$_0$ term with the other amplitudes.

2.4 *Search for* $\phi \to$*f*$_0\gamma$ *in* $\pi^+\pi^-\gamma$ *events.*

The search for $\phi \to$f$_0(\to \pi^+\pi^-)\gamma$ is characterized by the presence of high rate irreducible backgrounds due to the initial state radiation (ISR in the following), and to the process $e^+e^- \to \pi^+\pi^-\gamma$ either through the ϕ or through

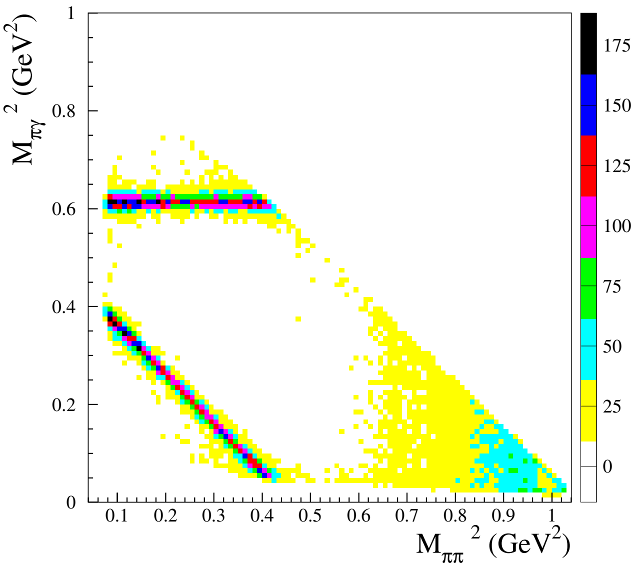

Fig. 3. Dalitz plot distribution for the selected sample of $\pi^0\pi^0\gamma$ events.

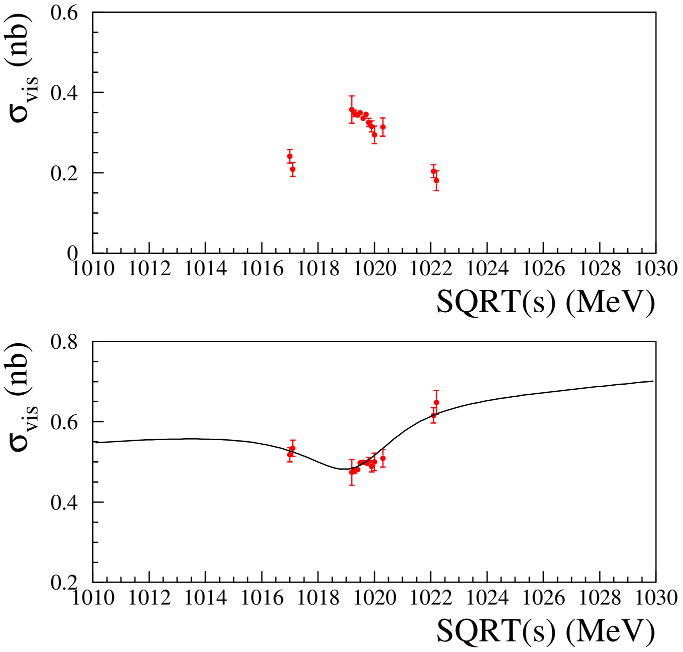

Fig. 4. Visible cross-section as a function of the center of mass energy $\sqrt{s}$ for events in the "f_0" region (upper plot) and events in the "$\omega\pi^0$" region (lower plot). In the lower plot the expected behavior due to the interference between the continuum and the ϕ decay (line) is also shown.

the ρ^0 tail (final state radiation, FSR in the following). A further lower rate background is due to the decay chain $\phi \rightarrow \rho^{\pm}(\rightarrow \pi^{\pm}\gamma)\pi^{\pm}$. Since the ISR cross-section is peaked at small photon angles respect to the beam line, the f_0 events are searched for in the large photon angle region $45^o < \theta < 135^o$. Although in this region the ISR is still the dominant process, the f_0 signal appears as a bump in the $\pi^+\pi^-$ invariant mass $M_{\pi\pi}$ spectrum around 980 MeV. Fig.5 shows the spectrum obtained at $\sqrt{s} = M_\phi$. The spectrum is dominated by the radiative return (ISR) to the ρ^0. The f_0 bump is clearly evident close to the high edge of the mass spectrum.

An overall fit to the spectrum has been done applying the following formula:

$$\frac{dN}{dM_{\pi\pi}} = \left[(\frac{d\sigma}{dM_{\pi\pi}})_{ISR} + (\frac{d\sigma}{dM_{\pi\pi}})_{FSR+f_0} + (\frac{d\sigma}{dM_{\pi\pi}})_{\rho\pi}\right] \times L \times \epsilon(M_{\pi\pi})$$

with L the integrated luminosity and $\epsilon(M_{\pi\pi})$ the selection efficiency function of $M_{\pi\pi}$. The ISR and $\rho\pi$ contributions are parametrized according to [10,12,13]. The FSR and f_0 contributions to the amplitude interfere with each other, since the two pion state has the same quantum numbers in both cases [14]. The f_0 amplitude is taken once more from the kaon-loop approach.

A fit of the whole spectrum is done with only 7 free parameters. Four of them are due to the pion form factor entering in the ISR term [12], the other 3 are the usual parameters entering in the kaon-loop model for the scalars, namely the scalar mass and the two couplings g_{f_0KK} and $g_{f_0\pi\pi}$. Moreover, the interference term is allowed to be either negative or positive [14]. A good fit is obtained (see fig.5) with background parameters in good agreement with values from [12] and with a sizeable negative interference between f_0 and FSR terms.

A forward-backward asymmetry

$$A = \frac{N^+(\theta > 90^o) - N^+(\theta < 90^o)}{N^+(\theta > 90^o) + N^+(\theta < 90^o)}$$

is expected, due to the C-odd term coming from the interference between FSR and ISR. Fig.6 shows the asymmetry as a function of $M_{\pi\pi}$ compared to the prediction based on the ISR-FSR interference alone. A significant deviation from the prediction is observed in the high mass region clearly due to the f_0 contribution.

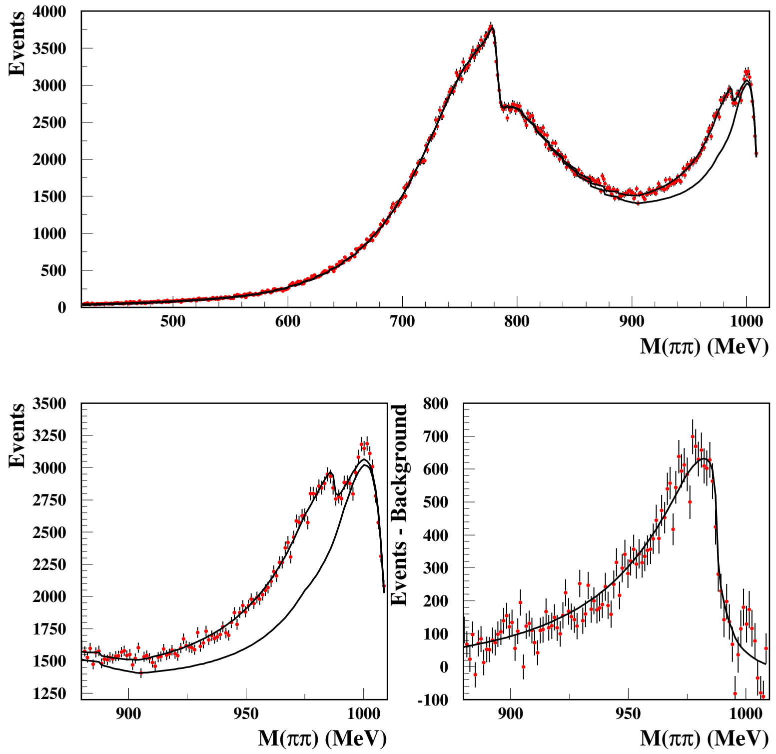

Fig. 5. **Top:** $M_{\pi\pi}$ spectrum of $\pi^+\pi^-\gamma$ events selected by requiring a photon at large angle. The upper (lower) curves are the result of the fit described in the text and the estimated background due to ISR, FSR and $\rho\pi$. **Bottom:** (left) enlarged view of the region of the "f_0" signal; (right) experimental spectrum after estimated background subtraction.

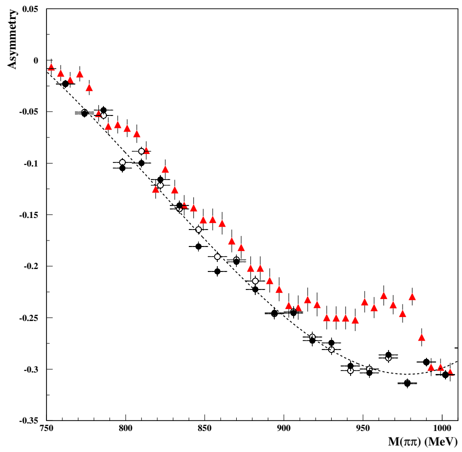

Fig. 6. Forward-Backward asymmetry A of $\pi^+\pi^-\gamma$ events as a function of $M_{\pi\pi}$. The curve and the black points are the Montecarlo expectations based on the interference between FSR and ISR only. The experimental data are reported as red triangles.

3 DAΦNE as an $\eta\,(\eta')$ factory

The Branching Ratio of the process $\phi \to \eta\gamma$ is about 1.3% [15]. This means that the total number of collisions accumulated at DAΦNE so far result in a clean, monochromatic sample of nearly 20 millions η mesons. KLOE can study with great detail both charged decay modes and fully neutral decay modes of the η. In fact the hermeticity of the detector allows precision studies of multiphotonic final states such as the chain $\phi \to \eta\gamma$ with $\eta \to \pi^0\,\pi^0\,\pi^0$ and seven photons in the final state, and the very good momentum resolution for charged tracks allows the study of the dynamics of three body decays such as $\eta \to \pi^+\,\pi^-\,\pi^0$ and $\eta \to \pi^+\,\pi^-\,\gamma$. The search for rare and not so rare decays of the η can be performed in a much cleaner environment than in dedicated hadron machines as well. The process $\phi \to \eta'\gamma$, while being about 500 times less probable than the $\phi \to \eta\gamma$ one, can still be used to test η' properties with unprecedented accuracy.

3.1 Dynamics of $\eta \to \pi^+\,\pi^-\,\pi^0$

The η is an isospin singlet and a pseudoscalar. Three pions in an angular momentum 0 configuration cannot have isospin zero, but isospin 1 is allowed. The $\eta \to \pi^+\,\pi^-\,\pi^0$ decay thus has to proceeded via isospin breaking and can take only place due to a finite mass difference m_d - m_u. The electromagnetic corrections to the decay are small (Sutherland 's theorem) and modify neither rate nor the Dalitz plot distributions noticeably.
Disregarding these, the decay amplitude at lowest order chiral perturbation theory (ChPT) is [16], [17]:

$$A(s,t,u) = \frac{1}{Q^2}\frac{m_K^2}{m_\pi^2}\left(m_\pi^2 - m_K^2\right)\frac{M(s,t,u)}{3\sqrt{3}F_0^2}$$

where

$$Q^2 \equiv \frac{m_s^2 - \hat{m}^2}{m_d^2 - m_u^2}$$

is a combination of quark masses and $\hat{m} = \frac{1}{2}\,(m_u + m_d)$ is the average u,d quark masses.
Thus the decay $\eta \to \pi^+\,\pi^-\,\pi^0$ can be used in order to determine the quantity Q^2. An investigation of the hadronic decay at leading order in ChPT yields a decay width which is significantly below the measured value

$$\Gamma^{theo}\left(\eta \to \pi^+ \pi^- \pi^0\right) = 66 \text{ eV}; \qquad \Gamma^{exp}\left(\eta \to \pi^+ \pi^- \pi^0\right) = 281 \pm 28 \text{ eV}.$$

The result is improved by performing a next-to-leading order calculation,

$$\Gamma^{theo}\left(\eta \to \pi^+ \pi^- \pi^0\right) \simeq 167 \pm 50 \text{ eV}.$$

but still fails to reproduce the phenomenological value. A new high statistics determination of the spectral shape is needed in order to determine whether the existing disagreement between experimental results and the theoretical predictions based on ChPT are caused by an inaccurate value for the $d - u$ quark mass difference or are due to the importance of higher order final state interaction effects.

The dynamics of the $\eta \to \pi^+ \pi^- \pi^0$ decay can be studied with the usual method of Dalitz plot analyses. The conventional variables X and Y are defined as:

$$X = \sqrt{3}\frac{T_+ - T_-}{Q_\eta} = \frac{\sqrt{3}}{2M_\eta Q_\eta}\,(u - t)$$

$$Y = \frac{3T_0}{Q_\eta} - 1 = \frac{3}{2M_\eta Q_\eta}\left[(m_\eta - m_{\pi^0})^2 - s\right] - 1$$

$$Q_\eta = m_\eta - 2m_{\pi^+} - m_{\pi^0}$$

where T_+, T_- and T_0 are the kinetic energies of the particles.

The measured distribution can then be fitted as:

$$|A(X,Y)|^2 \simeq (1 + aY + bY^2 + cX + dX^2 + eXY + ...)$$

C-parity conservation prevents odd powers in X being present in the expansion: thus parameters c and e should be zero. The experimental picture is still not clear, and PDG does not give averages of the parameters [15] since in all measurements performed so far any assumption made on quadratic terms changes significantly the result for the linear ones. We have fitted the probability density (see fig. 7) using the largest sample ever collected in the world, with more than 1.2 millions events in the Dalitz plot. Efficiency as function of X, Y is flat (see fig. 8) and amounts to about 36 % over the whole Dalitz plot; we exclude from the fit only the bins crossed by the kinematic boundaries. We confirm the absence of odd terms in X and obtain for the other parameters the results summarized in table 1. We notice that both quadratic terms in X and Y are needed to fit satisfactorily the observed distribution and, moreover,

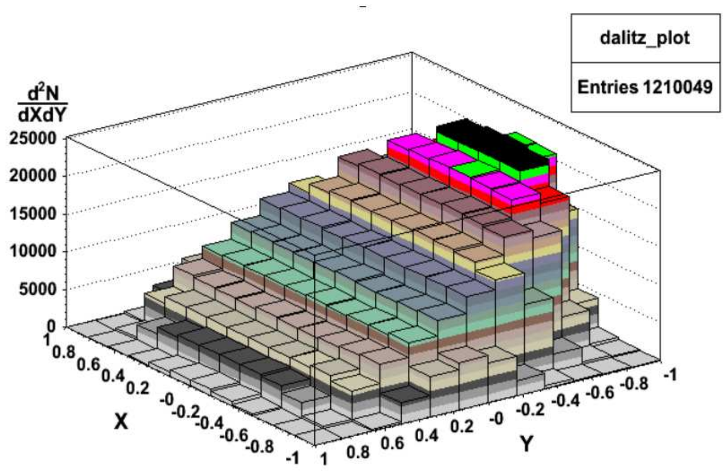

Fig. 7. The observed Dalitz plot distribution in $\eta \to \pi^+ \pi^- \pi^0$ events

that a sizeable cubic term in Y has to be taken into account (while we did not observe any sizeable X^2Y term). The evaluation of systematic effects is under completion: the background is completely irrelevant, since it accounts for about 0.7% of the observed distribution. The main systematic uncertainties are related to the binning choice, and are of same order of magnitude as the statistical ones.

$P(\chi^2)$	a	b	c	d	e	f
52%	$-1.075 \pm .008$	$.118 \pm .009$	$-.0005 \pm .004$	$.049 \pm .008$	$-.004 \pm .01$	$.13 \pm .02$
55%	$-1.075 \pm .008$	$.118 \pm .009$	$-.001 \pm .003$	$.049 \pm .009$	-	$.13 \pm .02$
59%	$-1.075 \pm .008$	$.118 \pm .009$	-	$.049 \pm .008$	-	$.13 \pm .02$
0	$-1.055 \pm .007$	$.102 \pm .009$	-	-	-	$.12 \pm .02$
0	$-1.020 \pm .004$	$.122 \pm .008$	$.046 \pm .008$	-	-	-

Table 1

Results of the fit to the $\eta \to \pi^+\pi^-\pi^0$ Dalitz plot density. The fit is performed with the function $1 + aY + bY^2 + cX + dX^2 + eXY + fY^3$ where X and Y are defined in the text.

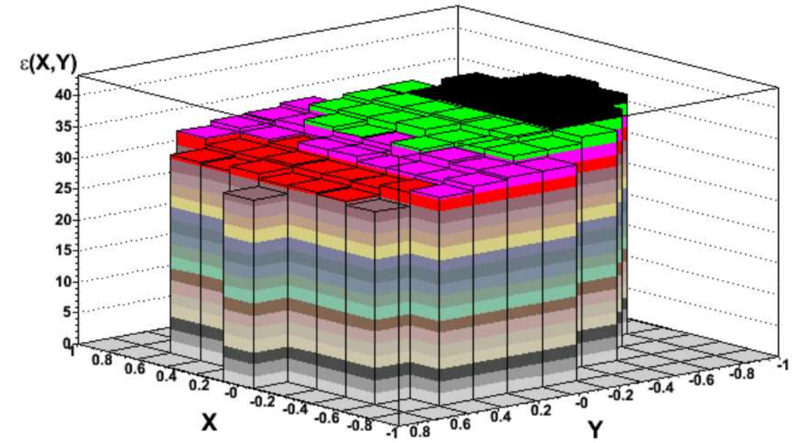

Fig. 8. Reconstruction efficiency for $\eta \to \pi^+ \pi^- \pi^0$ events

3.2 $\eta \to \pi^0\gamma\gamma$.

The $\eta \to \pi^0\gamma\gamma$ decay is interesting to test the Chiral Perturbation Theory prediction for the branching ratio and $m_{\gamma\gamma}$ spectrum. [18]. The most accurate measurement for the branching ratio[19] is, infact, far from any theoretical prediction for this decay based on ChPT. Recently a new measurement has been performed [20] giving a much lower value than the previous one, with a larger error. So it is unable to distinguish among several theoretical models. In the ChPT framework, the O(p^2) and O(p^4) terms give very small contributions to the BR of this decay [21] (of the order of 10^{-6}), for this reason terms of order p^6 and higher become important. The L_6 lagrangian has many terms, in order to constraint the values of coupling constants several approximations have been performed, ranging from resonance saturation assumption to large N_c effective theory. All of these give results quite similar and below the PDG value [22]. Many experiments have measured this branching ratio or have set an upper limit on it. The results of these experiments are shown in fig.9. As can be seen, the results spread over several order of magnitude, mainly due to an underestimate of $\eta \to \pi^0\pi^0\pi^0$ background. All these experiments were done at hadron machines, using mainly $\pi^- p \to \eta n$, and are largely dominated by $\pi^0\pi^0$ background and geometrical acceptance. KLOE performs a measurement

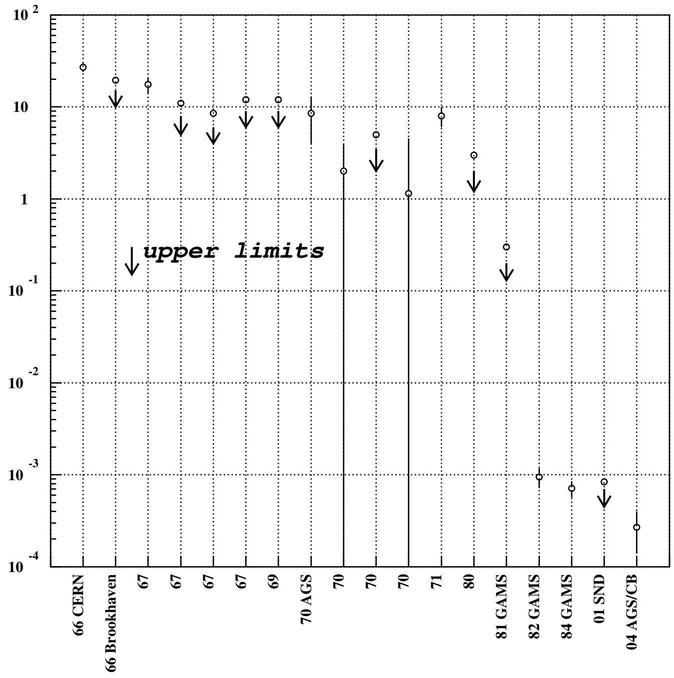

Fig. 9. Experimental measurements of $Br(\eta \to \pi^0\gamma\gamma)$ [20,22]

of competive precision in a cleaner environment. Furthermore, has different background topologies and experimental systematics.

The main steps for the search of this decay topology are described here:

(1) We require 5 clusters in the calorimeter whose $|t - r/c| < 5\sigma_t$, searching for $\phi \to \eta\gamma, \eta \to \pi^0\gamma\gamma, \pi^0 \to \gamma\gamma$ topology;
(2) we require cluster energies greater than 30 MeV and azimutal angles greater than 21° to reject fake clusters coming from machine background and suppress $e^+e^- \to \gamma\gamma$ background;
(3) after this selection we apply a kinematic fit with energy momentum conservation constraints in order to improve the resolution on the reconstructed energy of the photons;
(4) a second kinematic fit with the further constraint of the π^0 mass is performed and the χ^2 is retained as a selection variable;
(5) to suppress the $\gamma f_0(\to \pi^0\pi^0)$, $\gamma a_0(\to \eta\pi^0, \eta \to \gamma\gamma)$ and $e^+e^- \to \omega\pi^0(\omega \to \pi^0\gamma)$ background, a set of pseudo-χ^2 variables has been built, rejecting photons combination compatible with: $\pi^0\pi^0\gamma, \eta\pi^0\gamma, \omega(\to \pi^0\gamma)\pi^0$ hypothesis;
(6) to suppres $\eta \to \pi^0\pi^0\pi^0$ several techniques have been used. This background has several topologies. One can have five prompt clusters in the calorimeter if:
    (a) 2 clusters are lost, mostly at low azimutal angle;
    (b) 2 photons merge together in only one cluster and another one is lost,

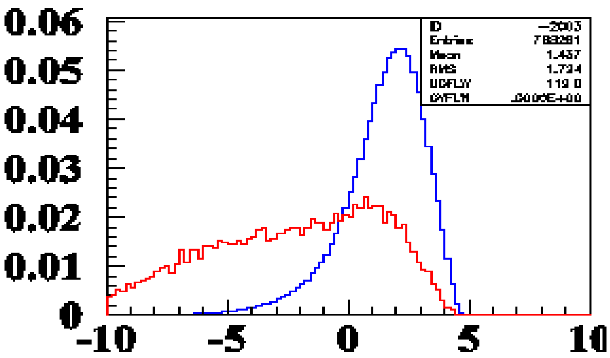

Fig. 10. log(likelihood) distribution for good clusters (blue, narrow) and merged ones (red, broad).

(c) two couple of photons are merged together into two clusters.
To reject case (a) a kinematic fit with also the momenta of the lost photons as free parameters has been performed, while for cases (b) and (c) a likelihood function, based on the shower shape variables, has been used to discriminate between good and merged clusters. In fig.10 the likelihood distribution both for good clusters and for merged ones has been shown.

With this selection we obtain an efficiency for the signal of 5.7%. To extract the signal from data we use the invariant mass of the least energetic 4 photons. The most energetic photon is, in fact, the photon coming from the electromagnetic decay $\phi \to \eta\gamma$ (363 MeV). To give an idea of the sensitivity, in fig.11 we compare our data together with MC prediction based on the $Br(\eta \to \pi^0\gamma\gamma)$ measured by the GAMS experiment. It is evident that our data are incompatible with GAMS measurement and are marginally in agreement with Crystall Ball published result. The background simulation and the efficiency for the signal is still under study.

3.3 $\eta \to \gamma\gamma\gamma$.

The $\eta \to 3\gamma$ decay is a C violating one. It is a sensitive test of C violation in the strong and electromagnetic interactions, KLOE has searched [23] for this decay in a sample of 19 million of η decays. The signal topology is a 4 photons one coming from the dacay chain $\phi \to \gamma\eta(\eta \to 3\gamma)$. There is only one background channel with exactly 4 photons in the final state, coming from $e^+e^- \to \gamma_{ISR}\omega(\to \pi^0\gamma)$, where γ_{ISR} is an Initial State Radiation photon. The presence of this background is evident in the $m_{\pi^0\gamma}$ distribution shown in fig.12. Other sources of background come from 5 clusters events in which one cluster is lost in acceptance, such as $e^+e^- \to \omega\pi^0$, $\phi \to \gamma f_0(\to \pi^0\pi^0)$ and $\phi \to \gamma a_0(\to \eta\pi^0)$. All these background sources are characterized by the

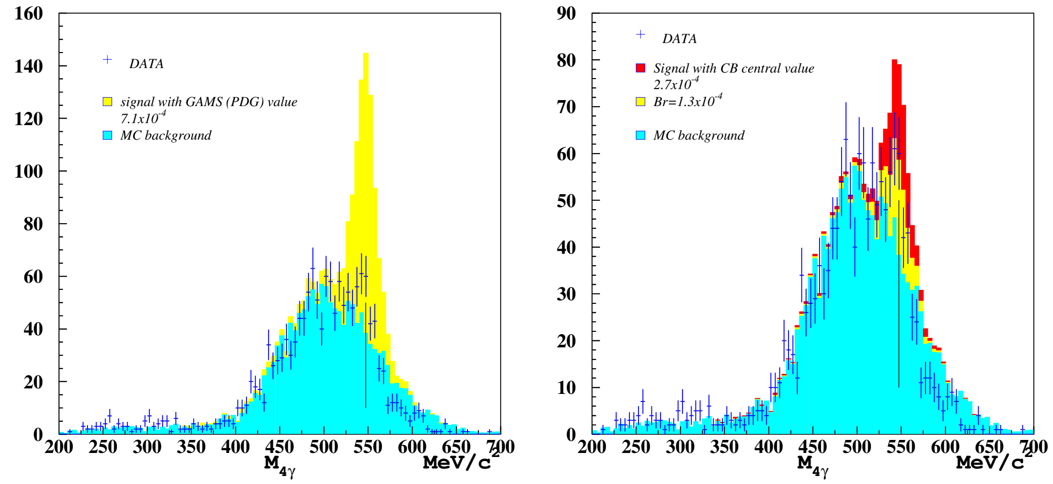

Fig. 11. M(4γ), the spectra expected from the GAMS and Crystall Ball measurement are shown. In the right plot we show also the expected spectrum for a $Br \sim 1/2$ of C.B. result.

presence of at least one π^0 in the final state. They all are rejected by cutting on 2-photon invariant mass. Residual background comes from events with < 4 photons, where a fake cluster coming from machine background or by the bad recostruction of a energy deposit into two clusters (splitting) adds up to the photons of the events. These events are rejected by requiring an high cluster energy (minimum cluster energy > 50 MeV) and a large azimutal angle $\theta_\gamma > 24.5°$. Starting from a sample of 19.8×10^6 η decays, 8268 events are left by the cuts. To search for $\eta \to 3\gamma$ events, we look for peaks in the distribution of the maximum energetic photons, that is shown both for data and MC in Fig.13. The background is estimated from data by fitting the side bands

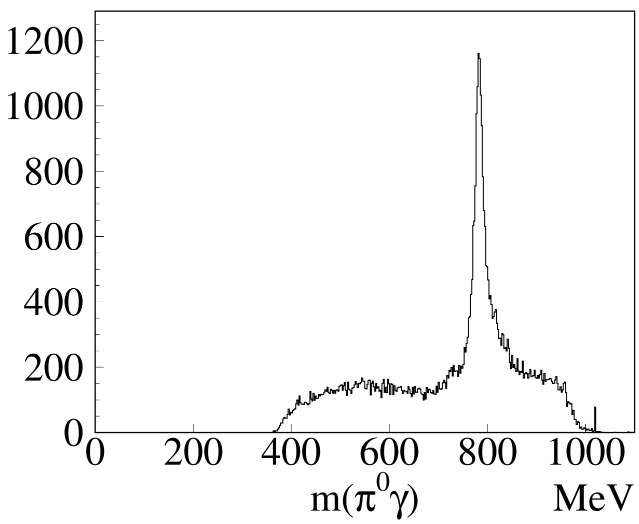

Fig. 12. $m_{\pi^0\gamma}$ distribution, is evident the peak at the ω mass showing the presence of $\omega\gamma$ background.

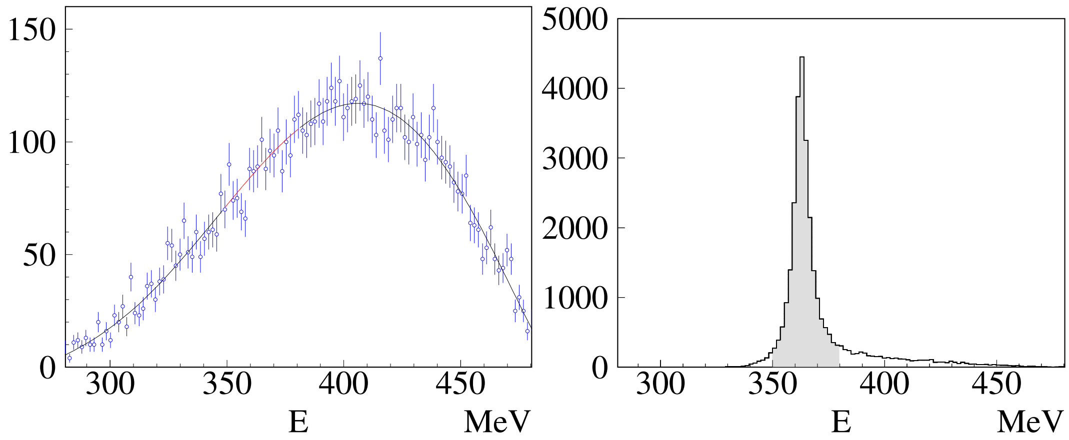

Fig. 13. Distribution of the maximum energy of the photons. The selection region for signal searching and the side bands region for background estimation are shown.

region shown in figure. By fitting this plot we find $N_{\eta\to 3\gamma} \leq 63.1$ @ 90% C.L., and using the selection efficiency $\epsilon = 20.0\% \pm 0.1\%(stat) \pm 0.6\%(syst)$ and the number of η decays expected (19789735) we obtain: $Br(\eta \to \gamma\gamma\gamma) \leq 1.6\times10^{-5}$ @90 % C.L.

This limit is the experimental best limit for this decay. The expected branching ratio from the Standard Model is $\leq 10^{-12}$ [24], so any discovery of a larger decay rate would be a clear signal of Standard Model deviation.

3.4 $\eta \to \pi^+\pi^-$.

The decay $\eta \to \pi^+\pi^-$ is a P and CP violating decay. The η is a pseudoscalar $J^{PC} = 0^{-+}$ state, the pions are also pseudoscalar states, so that any $\pi^+\pi^-$ system in a 0 angular momentum state has P=+1, C = +1 and CP=+1. This decay is allowed as a weak direct CP violating decay like $K_L \to \pi^+\pi^-$ but with a much lower branching ratio. According to Jarlskog and Shabalin [25] BR($\eta \to \pi^+\pi^-$)$\sim 10^{-27}$. The detection of this decay at an accessible level, should be a signal of P and CP violation in strong and/or electromagnetic interactions not explainable in the Standard Model framework.

The latest published [26] direct search of this decay has given the following 90% C.L. upper limit: $BR(\eta \to \pi^+\pi^-) < 3.3 \times 10^{-4}$ In this paper the preliminary result of a direct search of this decay with the KLOE detector is reported.

The signal is searched in the M(η) region of the $\pi^+\pi^-$ invariant mass spectrum of $\pi^+\pi^-\gamma$ events selected according to the $f_0(980)\to \pi^+\pi^-$ analysis described before. The η mass region is dominated by the initial state radiation with the low mass tail of the ρ^0. In this region the request of the photon at large angle ($45^o < \theta < 135^o$) strongly reduces the number of background events, with an acceptable loss of efficiency. From a Montecarlo simulation of the signal we estimate an overall efficiency on the signal ϵ_s=16.6%. The expected signal has a Gaussian shape with a mass resolution of 1.33 MeV. This value has been obtained by Monte Carlo simulation. To check the reproducibility of data by Monte Carlo, we have compared the same spectrum for $K_s \to \pi^+\pi^-$. The comparison is shown in fig.14 (left). Where a very good agreement can be seen.

Fig.14 (right) shows the measured $\pi^+\pi^-$ invariant mass spectrum in the region

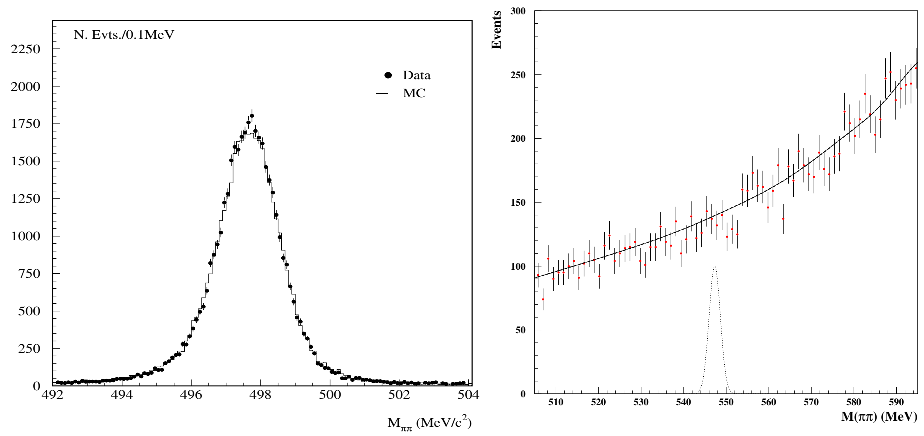

Fig. 14. **left** Data - Montecarlo comparison for the invariant mass distribution of $K_s \to \pi^+\pi^-$ decays. **right** mass spectrum between 500 and 600 MeV superimposed to the background without signal. The dotted curve is the expected signal shape in arbitrary units.

around the η mass. No signal is observed. In order to determine an upper limit, we have added to this background a Gaussian function representing the signal multiplied by a constant N_s. The Gaussian is normalised in such a way that N_s gives directly the integral of the function (number of signal events). The centre and the width of the Gaussian are fixed to 547.3 and 1.33 MeV respectively. We obtain: $N_s = -8 \pm 24$. The 90% confidence level upper limit on the number of events is obtained using the tables in [27]: $N_s < 32$. The branching ratio is $BR(\eta \to \pi^+\pi^-) = \frac{N_s}{\epsilon_s N_\eta}$ with N_η the number of η in the sample (1.43×10^7). The 90% C.L. upper limit is: $BR(\eta \to \pi^+\pi^-) < 1.3 \times 10^{-5}$. It improves by a factor ~ 30 the present best limit.

3.5 η - η' mixing

The η - η' system can be studied measuring the ratio:

$$R = \frac{\Gamma(\phi \to \eta'\gamma\ )}{\Gamma(\phi \to \eta\gamma\ )}$$

which had been measured previously by KLOE [28] using statistics collected in year 2000 and analyzing a chain with two charged pions and three photons in the final state. This ratio can be related to the pseudoscalar mixing angle in the flavor basis [29,30] and to the η' gluonic content [31,32]. This measurement was performed using about 120 signal events. From the newly collected statistics of year 2001-2002 we have analyzed a completely different final state, thus with different systematics and backgrounds, which proceeds via the decays: $\phi \to \eta' \gamma$; $\eta' \to \pi^+ \pi^- \eta$; $\eta \to \pi^0 \pi^0 \pi^0$ and the decays $\phi \to \eta' \gamma$; $\eta' \to \pi^0 \pi^0 \eta$; $\eta \to \pi^+ \pi^- \pi^0$. The final state is thus charachterized by two charged pions and seven photons, and has no physics background with the same topology in KLOE. After background subtraction (mainly from $\phi \to K_S K_L$ decays) we observe $3405 \pm 61 \pm 31$ $\phi \to \eta' \gamma$ events (see fig. 15,16). We normalize to the number of observed $\eta \to \pi^0 \pi^0 \pi^0$ decays in the same runs to obtain a preliminary measurement of the ratio of BR's :

$$R = (4.9 \pm 0.1_{stat} \pm 0.2_{syst}) \times 10^{-3}$$

where the systematic error is dominated by the knowledge of the intermediate BR's of the η' . This result compare favourably with our previous estimate [28] (which already dominates the world average [15]) but with considerably improved accuracy.

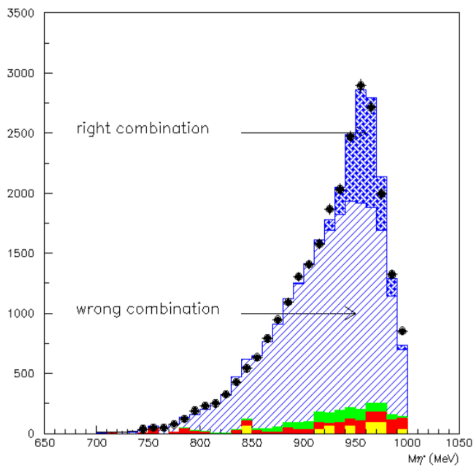

Fig. 15. The mass of all combinations of six photons and two tracks for $\phi \to \eta' \gamma$ candidate events. The contribution of right and wrong combinations for the signal, and from various $\phi \to K_S K_L$ decays (in green, yellow and red) is shown for Monte Carlo. Dots are data.

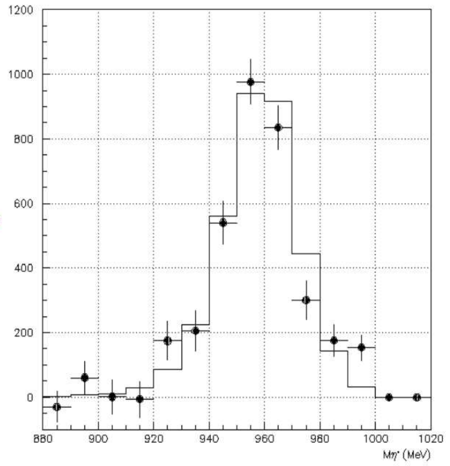

Fig. 16. The η' mass spectrum subtracted from combinatorial and physical background. Dots are data, continous line is from Monte Carlo.

4 A new measurement of the ϕ leptonic width.

KLOE has performed a new measurement of the ϕ leptonic widths Γ_{ll} with $l = e, \mu$ [33], using the two data samples taken below ($\sqrt{s}$=1017 MeV) and above ($\sqrt{s}$=1022 MeV) the ϕ peak together with the large amount of data taken at the ϕ peak. The dependences on $\sqrt{s}$ of the forward-backward asymmetry of Bhabha events A_{FB} and of the $e^+e^- \to \mu^+\mu^-$ cross-section $\sigma(\mu\mu)$ around the ϕ peak are sensitive to the value of Γ_{ee} and $\sqrt{\Gamma_{ee}\Gamma_{\mu\mu}}$ respectively. Fig.17 shows the measured values of A_{FB} as a function of $\sqrt{s}$. The three measured points allow us to evaluate three parameters: the ϕ mass M_ϕ, the forward-backward asymmetry at $W = M_\phi$ A^0_{FB}, and finally Γ_{ee}. The resulting curve is superimposed to the points, and the result for Γ_{ee} is:

$$\Gamma_{ee} = 1.32 \pm 0.05_{stat} \pm 0.03_{syst} \text{ keV}$$

$\sigma(\mu\mu)$ as a function of $\sqrt{s}$ is shown in Fig.18 together with the curve obtained by evaluating three parameters: the ϕ mass M_ϕ, the cross-section at the peak $\sigma_0(\mu\mu)$ and finally $\sqrt{\Gamma_{ee}\Gamma_{\mu\mu}}$. The result is:

$$\sqrt{\Gamma_{ee}\Gamma_{\mu\mu}} = 1.320 \pm 0.018_{stat} \pm 0.017_{syst} \text{ keV}$$

The two results are in good agreement consistently with lepton universality. Combining the two results we get:

$$\Gamma_{ll} = 1.320 \pm 0.017_{stat} \pm 0.015_{syst}\ keV$$

with a total uncertainty below 2 %. We point out that the value of Γ_{ee} is necessary for ϕ decay branching ratio measurements, and play also a role in the evaluation of the hadronic contribution to vacuum polarization [34].

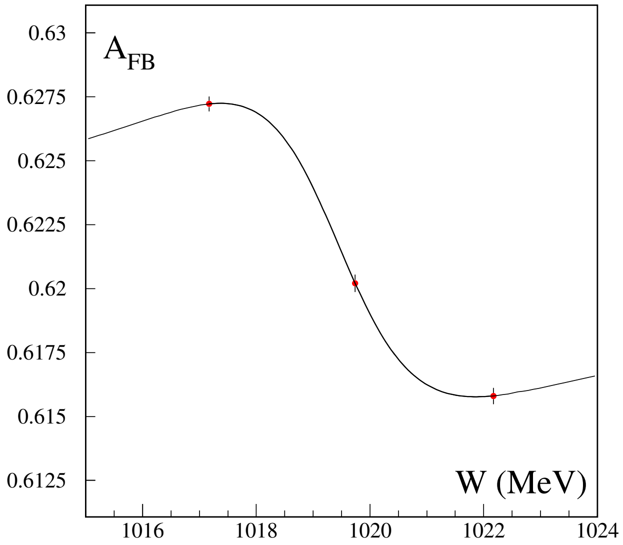

Fig. 17. Forward-Backward asymmetry A_{FB} of Bhabha events as a function of $W = \sqrt{s}$. The curve superimposed to the three measured points is obtained by evaluating the three parameters as described in the text.

5 Conclusions and outlook

A wide program of ϕ decays analyses is under way with the KLOE experiment based on a data sample of about 1.5×10^9 ϕ produced. A new insight on the low mass scalar mesons is provided by the study of $\pi\pi\gamma$ and $\eta\pi\gamma$ decays, while the η and η' produced through the $\phi \to \eta(\eta')\gamma$ decays, allows to extract relevant properties of the η meson, other than the η-η' mixing. A new accurate measurement of $\Gamma(\phi \to ll)$ is also obtained with a new method.

KLOE has now started a new period of data taking with the aim to increase by a factor 4 the present integrated luminosity.

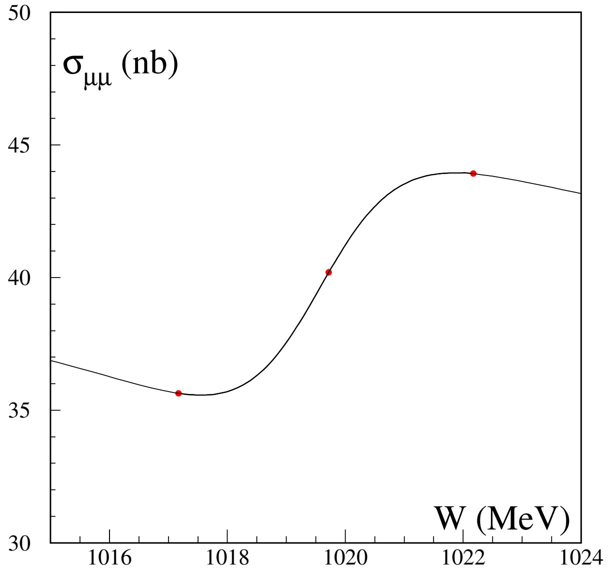

Fig. 18. $\mu^+\mu^-$ cross-section as a function of $W = \sqrt{s}$. Measured points and curve obtained.

References

[1] KLOE Coll., M. Adinolfi et al., Nucl. Instrum. Meth. A488 (2002) 51.

[2] KLOE Coll., M. Adinolfi et al., Nucl. Instrum. Meth. A482 (2002) 363.

[3] KLOE Coll., M. Adinolfi et al., Nucl. Instrum. Meth. A483 (2002) 649.

[4] KLOE Coll., M. Adinolfi et al., Nucl. Instrum. Meth. A492 (2002) 134.

[5] S. Guiducci, *Proc. of the 2001 Particle Accelerator Conf.*, P. Lucas, S. Webber (Eds.), Chicago, IL, U.S.A. (2001)

[6] N.Brown, F.Close, Second Dafne Physics Handbook, 2 (1995) 649; N.N.Achasov, V.N.Ivanchenko, Nucl.Phys. B315 (1989) 465; F.Close, A.Kirk, Phys.Lett.B515 (2001) 13;

[7] KLOE coll.,A. Aloisio et al., Phys.Lett.B536 (2002) 209;

[8] KLOE coll.,A. Aloisio et al., Phys.Lett.B537 (2002) 21;

[9] C.Amsler, N.A.Tornqvist, Phys.Rep.389 (2004) 61;

[10] N.N.Achasov, V.V.Gubin, Phys.Rev.D63 (2001) 094007;

[11] A.Bramon, A.Grau, G.Pancheri, Phys.Lett.B283 (1992) 416;

[12] J.H.Kühn, A.Santamaria, Z.Phys. C48 (1990) 45;

[13] F.Binner, J.H.Kühn, K.Melnikov, Phys.Lett.B459 (1999) 279;

[14] N.N.Achasov, V.V.Gubin, Phys.Rev.D57 (1998) 1987;

[15] K. Hagiwara et al., Phys. Rev. D66 (2002) 010001;

[16] J. Bijnens, J. Gasser Phys. Scripta T99 (2002) 39;

[17] B. Holstein Phys. Scripta T99 (2002) 55;

[18] J. Bijnens and J. Gasser, Phys. Scripta. T99 (2002) 34;

[19] Alde et al., Z.Phys. C25 (1984) 225;

[20] N. Knecht et al., Phys. Lett. B589 (2004) 14;

[21] L. Ameteller, Phys. Sript. T99 (2002) 45;

[22] M.N. Achasov et al., Nuc. Phys. B600 (2001) 3;

[23] KLOE Coll., A. Aloisio er al., Phys. Lett. B591 (2004) 49;

[24] P. Herczeg, *Proc. Int. Workshop on Production and Decay of Light Mesons*, P. Fleury ed., Paris, France, (World Scientific, 1988), 16;

[25] C.Jarlskog, E.Shabalin, Phys. Scripta T99,23 (2002); E.Shabalin in 'The Second Dafne physics handbook' pag.445 (1995);

[26] R.R. Akhmetshin et al., Phys.Lett. B462 (1999) 371 ;

[27] G.J. Feldman, R.D. Cousins, Phys. Rev. D57 (1998) 3873;

[28] A. Aloisio *et al.* [KLOE Collaboration], Phys. Lett. B541 (2002) 45;

[29] A. Bramon, R. Escribano and M. D. Scadron Phys. Lett. B503 (2001) 271;

[30] T. Feldmann, Int. Jou. Mod. Phys. A15 (2000) 159;

[31] J. L. Rosner Phys. Rev. D27 (1983) 1101;

[32] F. E. Close "Pseudoscalar mesons at DAΦNE" in "The DAΦNE physics handbook" vol. II (ed. L. Maiani, G. Pancheri and N. Paver, Frascati 1992);

[33] M. Antonelli, M.Dreucci, Leptonic decay widths of the phi-meson, KLOE note n. 193 (http://www.lnf.infn.it/kloe);

[34] S.Eidelman, F.Jegerlehner Z.Phys. C67 (1995) 585.